# Optical and photovoltaic properties of indium selenide thin films prepared by van der Waals epitaxy

J. F. Sánchez-Royo[a] and A. Segura
*Departament de Física Aplicada, Institut de Ciència dels Materials de la Universitat de València, c/Dr. Moliner 50, 46100 Burjassot, València, Spain*

O. Lang, E. Schaar, and C. Pettenkofer
*Hahn-Meitner-Institut, Abteilung Grenzflächen, Glienicker Strasse 100, 14109 Berlin, Germany*

W. Jaegermann
*Technische Universität Darmstadt, Fachbereich Materialwissenschaft, Fachgebiet Oberflächenforschung Petersen Strasse 23, D-64287 Darmstadt, Germany*

L. Roa and A. Chevy
*Laboratoire de Physique des Milieux Condensés, Université Pierre et Marie Curie, 4 place Jussieu, 75252 Paris, Cedex 05, France*

(Received 9 January 2001; accepted for publication 4 June 2001)

Indium selenide thin films have been grown on p-type gallium selenide single crystal substrates by van der Waals epitaxy. The use of two crucibles in the growth process has resulted in indium selenide films with physical properties closer to these of bulk indium selenide than those prepared by other techniques. The optical properties of the films have been studied by electroabsorption measurements. The band gap and its temperature dependence are very close to those of indium selenide single crystals. The width of the fundamental transition, even if larger than that of the pure single crystal material, decreases monotonously with temperature. Exciton peaks are not observed even at low temperature, which reveals that these layers still contain a large defect concentration. The current–voltage characteristic of indium selenide thin film devices was measured under simulated AM2 conditions. The solar conversion efficiency of these devices is lower than 0.6%. The high concentration of defects reduces the diffusion length of minority carriers down to values round to 0.2 $\mu$m. © *2001 American Institute of Physics.* [DOI: 10.1063/1.1389479]

## I. INTRODUCTION

Indium selenide (InSe) is a layered semiconductor that belongs to the III–VI family. Among these semiconductors, InSe is one of the most suitable for photovoltaic conversion because of its energy gap (1.3 eV) and its optical and transport properties.[1–3] The problem of the preparation of InSe high quality thin films is still unsolved due to the coexistence of several In–Se phases, that have been observed in films prepared by flash evaporation,[4–8] vacuum evaporation,[9–12] and by molecular beam epitaxy (MBE).[13–15] By these techniques, only polycrystalline or amorphous thin films containing nearly stoichiometric InSe have been obtained at certain critical conditions. Hall effect measurements in InSe thin films[5,7,8,16,17] show that carriers are mainly scattered by grain boundaries. The low electron mobility and its thermally activated behavior have been related to their polycrystalline structure. The optical properties of films prepared by these methods have been analyzed by means of absorption coefficient measurements.[4,6,7,9,10,18,19] The energy gap and the shape of the absorption edge are related to the amorphous or polycrystalline structure of these films. The absorption coefficient edge of polycrystalline films shows an exponential tail that has been explained by optical scattering at defects and grain boundaries and by extrinsic absorption due to a high concentration of defect states.[4,7] Photovoltaic effect has been studied only in compensated samples.[5] In this case the photovoltaic spectrum is governed by the presence of impurity centers and carrier traps, and the onset of the photovoltaic spectra is very different from that of bulk InSe.

The new possibilities opened by the so-called van der Waals (vdW) epitaxy[20,21] may be applied in the preparation of new thin film devices based on layered semiconductors even for large lattice mismatch.[22–27] The fact that InSe thin films prepared by this method show an epitaxial growth with the *c* axis perpendicular to the substrate and that InSe heterojunctions on other layered materials are nonreactive and exhibit atomically abrupt interfaces, support the high quality of these films with respect to those prepared by other techniques.[28–32]

In a previous article we analyzed the structural and photovoltaic properties of InSe thin films prepared by vdW epitaxy.[33] In that study, films were deposited by using crushed InSe single crystal inside a Knudsen cell as source material. Surface characterization of those films shows that they grow epitaxially with high crystalline quality, on the GaSe substrate. Additional indium precipitates seem to exist in the thickest films. The film contribution to the photovoltaic spectrum was related to its optical absorption edge. Due to the high concentration of defects in the films, the InSe exciton peak is not observed. In any case, the band gap and

[a]Electronic mail: jfsanche@uv.es

its temperature dependence appear to be quite close to those of InSe single crystals.

In this article we report on optical and photovoltaic properties of InSe thin films on GaSe single crystals, prepared by vdW epitaxy, using In and Se as source materials inside two Knudsen cells. In Sec. II we describe the experimental setup. The results obtained from the optical and photovoltaic measurements are shown in Sec. III. In Sec. IV we discuss the influence of defects on the optical and photovoltaic properties of the films and compare them with those of single crystals and films prepared by other methods.

## II. EXPERIMENT

The epitaxy of InSe thin films on GaSe was carried out in a MBE chamber equipped with Knudsen cells and a sample manipulator whose temperature could range from 150 to 900 K. Deposition fluxes were controlled by a quartz microbalance as well as by an ionization gauge mounted behind the sample holder. The base pressure in the growth and analysis chamber was $2\times10^{-10}$ mbar. More details of the system and experimental procedure may be found elsewhere.[28] The films were deposited on low resistivity *p*-GaSe substrates doped with N and Sn.[34,35] The substrates were carefully air cleaved with a razor blade in a plane parallel to the vdW plane. The thickness of the GaSe substrates was measured to be round to 40 $\mu$m from their infrared interference fringe pattern. After transfer into the growth chamber, the substrate was heated to 430 °C for 1 h to evaporate contaminations from the surface. Source materials were pure In and Se inside two $Al_2O_3$ Knudsen cells. InSe films were deposited at a nominal rate of 10 Å/min. The thickness ($d$) of the films ranged from $d=100$ to 1000 nm.

Indium tin oxide (ITO) and $In_2O_3$ films were used as transparent contacts on the InSe thin films.[3,36,37] The deposition of $In_2O_3$ layers was carried out *in situ* in a UHV chamber by reactive evaporation. The substrate temperature was 250 °C. ITO layers were deposited by dc reactive sputtering in an $Ar+O_2$ atmosphere from a 95% indium 5% tin cathode. The substrate temperature was 270 °C. The resistivity of $In_2O_3$ (ITO) films was measured to be of the order of $10^{-3}\,\Omega$ cm.

Low temperature electroreflectance measurements were carried out in a He closed cycle Leybold–Heraeus cryogenic system. For these measurements, an upper indium grid and a back indium contact were deposited on $In_2O_3$(ITO)/*n*-InSe/*p*-GaSe systems by vacuum evaporation. The optical source was a halogen burner with 3000 K radiation temperature. A Jobin-Ivon THR1000 infrared monochromator was used in order to obtain the electroreflectance spectra. Modulation was introduced by using a HP 8112A pulse generator at 1 kHz. The maximum voltage amplitude was 8 V. All devices were illuminated through the $In_2O_3$ (ITO) layer. The spectra were measured by using a lock-in amplifier and normalized to the reflectance spectra of the devices.

Current–voltage characteristic of the In/$In_2O_3$(ITO)/*n*-InSe/*p*-GaSe/In devices was measured under simulated AM2 conditions.

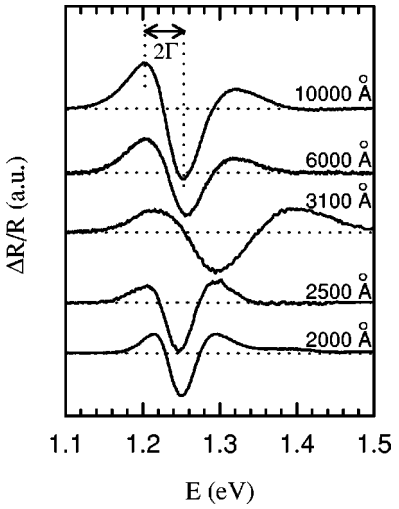


FIG. 1. Electroreflectance spectra measured by reflection at RT in several ITO/InSe/GaSe/In devices. The thickness of the corresponding InSe epilayer is indicated in the figure.

## III. RESULTS AND DISCUSSION

### A. Optical properties

Figure 1 shows the electroreflectance spectrum measured for several InSe thin films at room temperature (RT) in the energy range corresponding to the InSe absorption edge. All the spectra show a similar shape with a negative lobe between two positive ones. Nevertheless, from one sample to another, the width of the spectra (taken as $2\Gamma$ in Fig. 1) can change by a factor of 2 and the photon energy of the negative minimum can differ in 40 meV.

Let us first discuss the origin of the electroreflectance signal of our devices. In the conditions of our experiments, given the antireflective effect of ITO on the InSe films and the small reflectivity in the InSe/GaSe interface (due to the small refractive index difference), it is clear that the main contribution to the reflected signal, for photon energies lower than the GaSe band gap, comes from the back metallic contact, as shown in the inset of Fig. 2. This scheme also shows the barrier high ($V_n$) and its width ($w_n$) in the InSe side of the devices (the junction barrier is, obviously, in the *n*-InSe/*p*-GaSe interface). Taking into account that InSe thin films prepared on GaSe by vdW epitaxy show a band bending of $V_n=0.4$ eV,[30] the width of the barrier is expected to be round to $w_n=1000$ Å, for a donor concentration of $5\times10^{16}\,\mathrm{cm}^{-3}$, or even thinner due to the marked *n*-type behavior of these InSe films.[30,31] Therefore, the modulation field concentrates on the InSe/GaSe interface. Under these conditions, for photon energies close to the InSe band gap, the electroreflectance signal ($\Delta R/R$) of ITO($In_2O_3$)/InSe/GaSe/In devices can be expressed as

$$\frac{\Delta R}{R}=2d\Delta\alpha, \tag{1}$$

where $\Delta\alpha$ is the InSe modulated absorption coefficient. Equation (1) implies that electroreflectance measurements in these devices correspond to electroabsorption measurements by reflection. This is in opposition to that observed in elec-

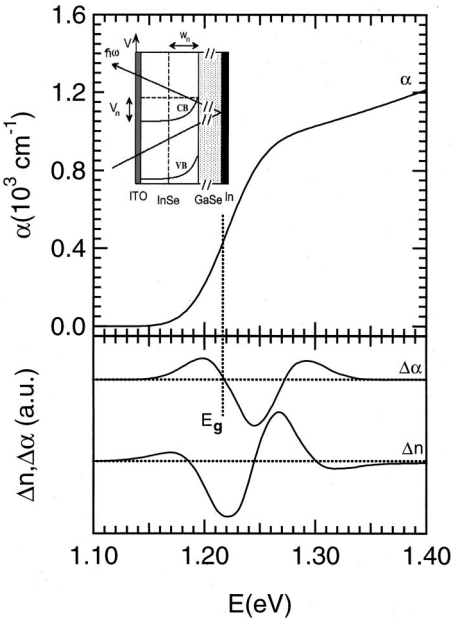


FIG. 2. Modulated absorption coefficient and refractive index calculated from the absorption coefficient edge of an InSe thin film of 2500-Å-thick at RT following the Aspnes' third derivative rule. The inset illustrates the experimental configuration of the electroreflectance measurements. The energy diagram of the InSe conduction (CB) and valence (VB) bands is included. The height ($V_n$) and the width ($w_n$) of the potential barriers are also indicated.

troreflectance measurements carried out in ITO/$p$-InSe single crystal devices, which mostly reflect modulation of the real part of the refractive index ($\Delta n$).[38] In order to check this hypothesis, we have carried out electroabsorption measurements at RT in transmission configuration in a $In_2O_3$/InSe/GaSe/In device, in which the thickness of the InSe thin film is 2500 Å, reproducing the electroreflectance spectrum measured at this temperature.[38]

To go further in this idea, we show in Fig. 2 $\Delta n$ and $\Delta\alpha$ calculated from the absorption coefficient edge of an InSe thin film,[33] following the Aspnes' third derivative rule.[39] In this figure, the position of the energy gap ($E_g$) has been pointed out. As one can observe, the shape of the calculated spectrum of $\Delta n$ clearly differs from that obtained from electroreflectance measurements. Nevertheless, the calculated spectrum of $\Delta\alpha$ satisfactorily reproduces the behavior of the experimental spectra (Fig. 1).

In order to analyze the optical properties of the InSe films prepared by vdW epitaxy, we have recorded the electroreflectance (electroabsorption) spectrum for several InSe thin films in the energy range of the InSe absorption edge as a function of temperature. The behavior observed in these spectra is similar for all samples here studied. Figure 3 shows the electroreflectance spectra for a 2000-Å-thick InSe thin film device in the temperature range from 300 to 60 K. At lower temperature the electroreflectance signal tends to vanish for all films. In these spectra the characteristic shift to higher energy of the absorption edge with lowering temperature can be clearly observed. Dotted lines in Fig. 3 indicate the position, at different temperatures, of the lower energy

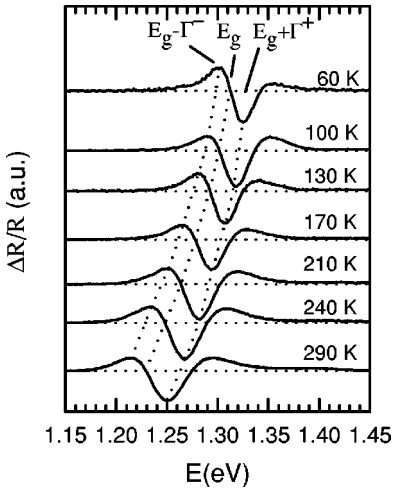


FIG. 3. Electroreflectance spectra measured in an ITO/InSe/GaSe/In device with a 2000-Å-thick InSe epilayer, in the temperature range from 300 to 60 K. The temperature evolution of $E_g$, $E_g+\Gamma^+$ and $E_g-\Gamma^-$ is followed in the figure by dotted lines.

maximum ($E_g-\Gamma^-$), the band gap $E_g$, and the higher energy minimum ($E_g+\Gamma^+$).

Figure 4(a) shows the shift of $E_g$ with temperature as obtained from the electroreflectance spectra for different InSe thin film devices. The values of $E_g$ are referred to that obtained at RT for each sample [$E_g(300\,\mathrm{K})=1.229$, 1.222 and 1.232 eV for devices with a 2000-, 2500- and 6000-Å thick InSe film, respectively]. As one can see, the shift of $E_g$ is linear in the temperature range from 150 to 300 K, with a temperature coefficient of $dE_g/dT=-0.37\pm0.02$ meV/K. However, the temperature coefficient of $E_g$ decreases in absolute value at temperature lower than 150 K. Figure 4(b) shows the temperature dependence of both half width $\Gamma^+$ and $\Gamma^-$. The behavior of both half widths is different from each other. The half width $\Gamma^+$ behavior is similar for all InSe

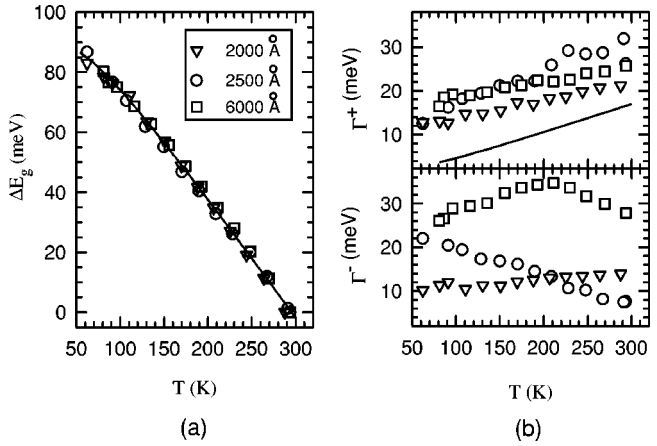


FIG. 4. (a) Temperature dependence of the band gap obtained for different ITO/InSe/GaSe/In devices as obtained from electroreflectance measurements. The thickness of the corresponding InSe epilayer is indicated in the figure. The solid line is a fit of the electron–phonon model to the experimental data. (b) Temperature dependence of $\Gamma^+$ and $\Gamma^-$. Symbols follow the same meaning as that in (a). Solid line corresponds to temperature dependence of the half width of the excitonic peak measured in InSe single crystal.

films measured, decreasing monotonously with temperature. Nevertheless, the half width $\Gamma^-$ behavior shows a larger dispersion among samples.

Camassel *et al.*[40] studied the optical properties of InSe single crystal through absorption coefficient measurements. These authors observed a linear dependence of $E_g$ with temperature between 300 and 150 K, with a temperature coefficient of $dE_g/dT = -0.37$ meV/K. At temperatures lower than 150 K the band gap tended to a constant value of $E_g(0) = 1.352$ eV. In that work, the temperature dependence of the band gap was analyzed and reproduced considering the interaction of electrons at the bottom of the conduction band with 14.5 meV optical phonons. In our films, the observed temperature dependence of the band gap [Fig. 4(a)] suggests that electron–phonon interaction is also responsible for this behavior. The solid line in Fig. 4(a) corresponds to the expected band gap temperature dependence determined by the 14.5 meV optical phonon,[40] with $E_g(0) = 1.317 \pm 0.003$ eV and $B = 18.1 \pm 0.2$ meV$^{1/2}$ ($B$ is a normalization constant defined in Ref. 40). We have obtained a good agreement with experimental results, which indicates that the intrinsic properties of these epilayers are those of InSe single crystal.

With regard to the width of the optical transition, the different behavior observed between $\Gamma^+$ and $\Gamma^-$ can be related to the fact that the high-energy side of the electroreflectance spectra corresponds to band to band transitions, modified by the continuum of the electron-hole interaction. Opposite to this, the low-energy side of the spectra is determined by the density of states tail, quite more sensitive to defect presence. These arguments are supported by the behavior exhibited by $\Gamma^+$. In Fig. 4(b) we have included the temperature dependence of the Lorentzian half width at half maximum of the excitonic peak obtained from absorption coefficient measurements in InSe single crystals [solid line in Fig. 4(b)].[40] As one can observe, this curve exhibits a similar dependence to that obtained for $\Gamma^+$ from electroreflectance measurements in InSe thin films prepared by vdW epitaxy. This fact suggests that, despite the presence of defects that reduces the lifetime of exciton in these thin films, the defect concentration is low enough to allow observing the phonon contribution to the determination of the width of the optical transition. In this way, the temperature dependence of $\Gamma^+$ could be interpreted as the intrinsic contribution, due to optical phonons, plus a nearly constant term of 10–15 meV due to defect contribution. The defect contribution is specially effective in the low-energy side of the electroreflectance spectra, in which exciton peak is usually observed. For this reason, it is not observable even at low temperature.

### B. Current–voltage characteristic and solar efficiency

Photovoltaic spectra of the $In_2O_3$/InSe/GaSe:N/In devices will not be discussed here as they are very similar to those reported in Ref. 33. Figure 5 shows the $I(V)$ characteristic of one of these devices, with a 2500-Å-thick InSe film, in the dark and under simulated AM2 conditions. We have also included its $I(V)$ characteristic under AM2 conditions filtering the light of wavelength shorter than 680 nm, in order to eliminate the contribution of the GaSe substrate to the photocurrent.

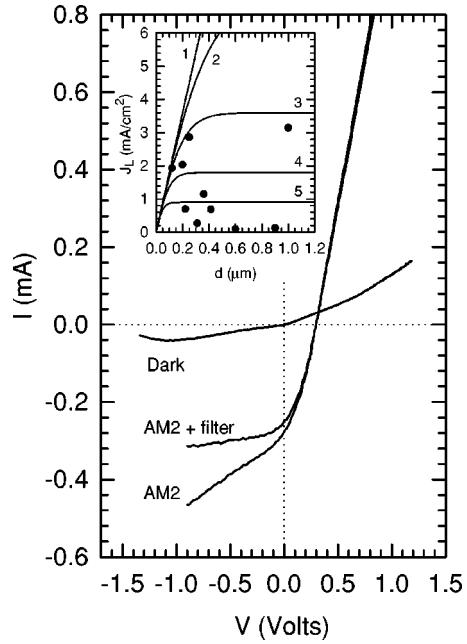


FIG. 5. $I(V)$ characteristic under dark and simulated AM2 conditions of an ITO/InSe/GaSe/In device with a 2500-Å-thick InSe epilayer, measured at RT. The $I(V)$ characteristic measured under AM2 conditions filtering the GaSe substrate contribution is also included. The inset shows $J_L$ of several ITO/InSe/GaSe/In devices measured under AM2 conditions (closed circles). Solid lines correspond to maximum photocurrent density calculated for different values of diffusion length of minority carrier. Curve 1 corresponds to $L_p \gg d$. Curves from 2–5 correspond to $L_p = 0.4$, 0.2, 0.1, and 0.05 $\mu$m, respectively.

Table I shows the photocurrent density ($J_L$) and the photovoltage ($V_{oc}$) values obtained of $I(V)$ characteristic measurements in different $In_2O_3$(ITO)/InSe/GaSe:N,Sn/In devices. These devices give photovoltages of $V_{oc} = 0.2–0.3$ eV and photocurrents up to $J_L = 3$ mA/cm$^2$, which are considerably higher than those obtained of InSe thin films prepared by using one crucible.[38] The filling factor (FF) is of the order of 0.2–0.4, which implies that there is a considerable loss of photocurrent in these devices as a result of their large series resistance. Table I also shows the solar efficiency values ($\eta$) obtained of these devices, which are lower than $\eta = 0.6\%$. Nevertheless, these results can be ex-

TABLE I. Efficiency parameters obtained for several InSe thin film solar cells.

| $d$ (Å) | $V_{oc}$ (V) | $J_L$ (mA/cm$^2$) | FF | $\eta$ (%) |
|---|---|---|---|---|
| 1200 | 0.220 | 1.93 | 0.30 | 0.36 |
| 2000 | 0.327 | 2.03 | 0.20 | 0.39 |
| 2200 | 0.173 | 0.69 | 0.20 | 0.06 |
| 2500 | 0.286 | 2.86 | 0.20 | 0.40 |
| 3100 | 0.168 | 0.27 | 0.25 | 0.03 |
| 3600 | 0.281 | 1.53 | 0.30 | 0.36 |
| 4150 | 0.181 | 0.68 | 0.15 | 0.05 |
| 6000 | 0.295 | 0.10 | 0.40 | 0.03 |
| 10 000 | 0.334 | 3.14 | 0.20 | 0.59 |

plained taking into account that the main contribution to photocurrent comes from the $n$-side of the InSe/GaSe heterojunction, as one can see in $I(V)$ characteristic measurements filtering the GaSe contribution (Fig. 5).

Under the assumption that photocurrent is mainly generated in the InSe epilayer, one can estimate the maximum photocurrent generated in these devices. For such thin layers, even at 1 eV above the band gap the product of the InSe absorption coefficient ($\alpha$) and the InSe epilayer thickness ($d$) would be lower than 0.25. Therefore, the photocurrent density can be expressed as[41]

$$J_L \approx q(1-R)L_p \tanh\left(\frac{d}{L_p}\right)\int_{E_g}^{\infty}\Phi_0(E)\alpha(E)dE, \qquad (2)$$

where $q$ is the electron charge, $L_p$ is the diffusion length of minority carriers, and $\Phi_0(E)$ is the photon flux density. The integral in Eq. (2) has been numerically evaluated. The inset of Fig. 5 shows the photocurrent measured in $In_2O_3$(ITO)/InSe/GaSe:N,Sn/In devices with InSe films of different thickness, under illumination. We have also included the curves calculated through Eq. (2) for different values of $L_p$ (solid lines in this inset). As one can observe, the value of photocurrent obtained in some of the thinner InSe thin film devices is close to the maximum one (curve 1). On the contrary, photocurrent shows lower values for thicker InSe thin film devices. These facts suggest that the diffusion length of minority carriers is clearly lower than the InSe thin film thickness in these devices, coherently with the fact that the defect presence is more pronounced in thicker InSe films. In these films the value of $L_p$ is of the order of $L_p = 0.05\,\mu$m, being of the order of $L_p = 0.2\,\mu$m in those with lower defect concentration.

## IV. CONCLUSIONS

We have prepared InSe thin films on GaSe substrates by vdW epitaxy from independent In and Se sources. The use of two crucibles in the growth process results in InSe thin films with physical properties closer to InSe single crystal than those prepared by using one single InSe source.

Electroabsorption measurements by reflection as a function of temperature reflect the behavior of the direct optical transition. These measurements allowed us to analyze the temperature dependence of the band gap and the width of the optical transition. The temperature dependence of band gap has been analyzed in the frame of a model that includes electron–phonon interaction. As in InSe single crystal, the phonon involved in this interaction is the 14.5 meV homopolar phonon. The temperature dependence of the width of transition shows a similar behavior to that observed in InSe single crystal, decreasing monotonously with temperature.

$I(V)$ characteristics of $In_2O_3$(ITO)/InSe/GaSe:N,Sn/In devices have been analyzed. The photocurrent density and photovoltage of the best devices reach values of $J_L = 3\,\text{mA/cm}^2$ and $V_{oc} = 0.3\,\text{V}$, respectively. The solar conversion efficiency of these devices is lower than $\eta = 0.6\%$. The high concentration of defects reduces the diffusion length of minority carriers down to values round to $L_p = 0.2\,\mu$m.


[1] A. Segura, J. P. Guesdon, J. M. Besson, and A. Chevy, Rev. Phys. Appl. **14**, 253 (1979).
[2] A. Segura, J. P. Guesdon, J. M. Besson, and A. Chevy, J. Appl. Phys. **54**, 876 (1983).
[3] J. Martínez-Pastor, A. Segura, J. L. Valdés, and A. Chevy, J. Appl. Phys. **62**, 1477 (1987).
[4] J. P. Guesdon, C. Julien, M. Balkanski, and A. Chevy, Phys. Status Solidi A **101**, 495 (1987).
[5] J. P. Guesdon, B. Bobbi, C. Julien, and M. Balkanski, Phys. Status Solidi A **102**, 327 (1987).
[6] C. Julien, N. Benramdane, and J. P. Guesdon, Semicond. Sci. Technol. **5**, 905 (1990).
[7] N. Benramdane, J. P. Guesdon, and C. Julien, Phys. Status Solidi A **146**, 675 (1994).
[8] C. Julien, A. Khelfa, N. Benramdane, and J. P. Guesdon, J. Mater. Sci. **30**, 4890 (1995).
[9] S. K. Biswas, S. Chaudhuri, and A. Choudhury, Phys. Status Solidi A **105**, 467 (1988).
[10] B. Thomas and T. R. N. Kutty, Phys. Status Solidi A **119**, 127 (1990).
[11] Y. Igasaki, H. Yamauchi, and S. Okamura, J. Cryst. Growth **112**, 797 (1991).
[12] S. Marsillac, J. C. Bernède, and A. Conan, J. Mater. Sci. **31**, 581 (1996).
[13] J. Y. Emery, C. Julien, M. Jouanne, and M. Balkanski, Appl. Surf. Sci. **33,34**, 619 (1988).
[14] J. Y. Emery, L. Brahim-Otsmane, C. Herlemann, and A. Chevy, J. Appl. Phys. **71**, 3256 (1992).
[15] L. Brahim-Otsmane, J. Y. Emery, and M. Eddrief, Thin Solid Films **237**, 291 (1994).
[16] G. Micocci, A. Tepore, R. Rella, and P. Siciliano, Sol. Energy Mater. **22**, 215 (1991).
[17] M. Parlak, Ç. Erçelebi, I. Günal, Z. Salaeva, and K. Allakhverdiev, Thin Solid Films **258**, 86 (1995).
[18] N. Banerjee, B. K. Samantaray, and A. K. Chaudhuri, J. Mater. Sci. **13**, 1443 (1994).
[19] J. C. Bernède, S. Marsillac, A. Conan, and A. Godoy, J. Phys.: Condens. Matter **8**, 3439 (1996).
[20] A. Koma, Thin Solid Films **216**, 72 (1992).
[21] W. Jaegermann, *Surface Studies of Layered Materials in Relation to Energy Converting Interfaces*, in *Photoelectrochemistry and Photovoltaics of Layered Semiconductors*, edited by A. Aruchamy (Kluwer, Dordrecht, 1984).
[22] K. Ueno, T. Shimada, K. Saiki, and A. Koma, Appl. Phys. Lett. **4**, 327 (1990).
[23] K. W. Nebesny, and N. R. Armstrong, Chem. Mater. **3**, 829 (1991).
[24] K. Ueno, T. Shimada, K. Saiki, and A. Koma, Surf. Sci. **267**, 43 (1992).
[25] T. Shimada, F. S. Ohuchi, and B. A. Parkinson, J. Vac. Sci. Technol. A **10**, 539 (1992).
[26] J. Y. Emery, L. Brahin-Otsmane, M. Eddrief, C. Gebenne, and M. Balkanski, Appl. Surf. Sci. **65/66**, 661 (1993).
[27] R. Schlaf, S. Tiefenbacher, O. Lang, C. Pettenkofer, and W. Jaegermann, Surf. Sci. **303**, L343 (1994).
[28] O. Lang, R. Schlaf, Y. Tomm, C. Pettenkofer, and W. Jaegermann, J. Appl. Phys. **75**, 7805 (1994).
[29] O. Lang, Y. Tomm, R. Schlaf, C. Pettenkofer, and W. Jaegermann, J. Appl. Phys. **75**, 7814 (1994).
[30] O. Lang, A. Klein, C. Pettenkofer, W. Jaegermann, and A. Chevy, J. Appl. Phys. **80**, 3817 (1996).
[31] A. Klein, O. Lang, R. Schlaf, C. Pettenkofer, and W. Jaegermann, Phys. Rev. Lett. **80**, 361 (1998).
[32] M. Budiman, A. Yamada, and M. Konagai, Jpn. J. Appl. Phys., Part 1 **37**, 4092 (1998).
[33] J. F. Sánchez-Royo, A. Segura, O. Lang, C. Pettenkofer, W. Jaegermann, A. Chevy, and L. Roa, Thin Solid Films **307**, 283 (1997).
[34] J. F. Sánchez-Royo, A. Segura, A. Chevy, and L. Roa, J. Appl. Phys. **79**, 204 (1996).
[35] J. F. Sánchez-Royo, D. Errandonea, A. Segura, L. Roa, and A. Chevy, J. Appl. Phys. **83**, 4750 (1998).
[36] T. A. Hessert, X. Li, M. W. Wanlass, A. J. Nelson, and T. J. Coutss, J. Vac. Sci. Technol. A **8**, 1912 (1990).
[37] M. A. Martínez, J. Herrero, and M. T. Gutiérrez, Thin Solid Films **269**, 80 (1995).

[38] J. F. Sánchez-Royo, thesis, Universidad de Valencia, 1998.
[39] D. E. Aspnes, *Modulation Spectroscopy, Electric Field effects on the Dielectric Function of Semiconductors*, in *Handbook of Semiconductors*, edited by M. Balkanski (North-Holland, Amsterdam, 1980), Vol. 2.
[40] J. Camassel, P. Merle, H. Mathieu, and A. Chevy, Phys. Rev. B **17**, 4718 (1977).
[41] S. M. Sze, *Physics of Semiconductor Devices*, 2nd ed. (Wiley, New York, 1981).